

Investigation on synthesis and physical properties of metal doped picene solids

Takashi Kambe,^{1*} Xuexia He,² Yosuke Takahashi,¹ Yusuke Yamanari,¹ Kazuya Teranishi,² Hiroki Mitamura,², Seizi Shibasaki,¹ Keitaro Tomita,¹ Ritsuko Eguchi,² Hidenori Goto,^{2,6} Yasuhiro Takabayashi,² Takashi Kato,³ Akihiko Fujiwara,⁴ Toshikaze Kariyado,⁵ Hideo Aoki,⁵ and Yoshihiro Kubozono^{2,6*}

¹Department of Physics, Okayama University, Okayama 700-8530, Japan

²Research Laboratory for surface Science, Okayama University, Okayama 700-8530, Japan

³Institute for Innovative Science and Technology, Graduate School of Engineering, Nagasaki Institute of Applied Science, Nagasaki 851-0121, Japan

⁴Japan Synchrotron Radiation Research Institute, SPring-8, Hyogo 679-5198, Japan

⁵Department of Physics, The University of Tokyo, Tokyo 113-0033, Japan

⁶Research Centre of New Functional Materials for Energy Production, Storage and Transport, Okayama University, Okayama 700-8530, Japan

PACS number; [74.70.Wz, 74.70.Kn, 74.62.Fj, 74.62.Bf]

(Received: 26 September 2012)

We report electronic structure and physical properties of metal doped picene as well as selective synthesis of the phase exhibiting 18 K superconducting transition. First, Raman scattering is used to characterize the number of electrons transferred from the dopants to picene molecules. The charge transfer leads to a

softening of Raman scattering peaks, which enables us to determine the number of transferred electrons. From this we have identified that three electrons are transferred to each picene molecule in the superconducting doped-picene solids. Second, we report the pressure dependence of T_c in 7 and 18 K phases of K_3 picene. The 7 K phase shows a negative pressure-dependence, while the 18 K phase exhibits a positive pressure-dependence which cannot be understood with a simple phonon mechanism of BCS superconductivity. Third, we report a new synthesis method for superconducting K_3 picene by a solution process with monomethylamine, CH_3NH_2 . This method enables one to prepare selectively the K_3 picene sample exhibiting 18 K superconducting transition. The discovery of suitable way for preparing K_3 picene with $T_c = 18$ K may facilitate clarification of the mechanism of superconductivity.

Corresponding author: Takashi Kambe, kambe@cc.okayama-u.ac.jp & Yoshihiro Kubozono, kubozono@cc.okayama-u.ac.jp

I. Introduction

Recently a new class of organic superconductors has been discovered in aromatic systems. They are solids of hydrocarbons that include picene, coronene, phenanthrene and 1,2:8,9-dibenzopentacene,¹⁻⁶ doped with metal atoms. First, the superconductivity was discovered in potassium-doped picene, $K_3\text{picene}$, which showed two different superconducting transition temperatures, one with $T_c = 7$ K and the other as high as 18 K.¹ This has been followed by other studies, and the highest T_c among these hydrocarbon superconductors to date attains to be 33 K observed in $K_{3.45}\text{dibenzopentacene}$,⁶ whose T_c is much higher than the highest T_c (14.2 K at 8.2 GPa⁷ in β' - (BEDT-TTF)₂ICl₂) in charge-transfer organic superconductors. Thus the hydrocarbon superconductors are very attractive from viewpoints of development of new high- T_c superconductors as well as fundamental physics of superconductivity. Theoretical calculations for picene superconductors were also achieved, which suggests that the electron-phonon coupling is strong,^{8,9} the conduction band comprises four bands arising from two LUMO orbitals,¹⁰ and strong hybridization between the dopants and molecules invalidates a rigid-band picture¹⁰. The departure from the rigid band picture was experimentally evidenced by photoemission spectroscopy.¹¹ Very recently, specific heat measurements were achieved for $Ba_{1.5}\text{phenanthrene}$,^{12,13} which suggests a s-wave, single superconducting gap and intermediate electron-phonon coupling strength.

The T_c for the solid $K_3\text{picene}$ was found to be either 7 or 18 K,^{1,2} while the T_c of $K_3\text{phenanthrene}$ was reported to be only ~ 5 K.³ Donation of three electrons to aromatic hydrocarbon molecule was reported to be a key for superconductivity.¹⁻⁶ The nominal x value in the superconducting samples of $A_x\text{hydrocarbon}$, $AE_x\text{hydrocarbon}$ and $Ln_x\text{hydrocarbon}$ (A: alkaline-metal atom, AE: alkaline-earth metal atom, Ln: lanthanide atom) are $x = 3, 1.5$ and 1, respectively. It is imperative to determine the real x value (number of metal atoms intercalated) in these hydrocarbon solids. Rietveld refinements for X-ray powder diffraction patterns have been extensively used for determining x value in metal-doped C_{60} compounds.¹⁴⁻¹⁶ Since the single crystals cannot simply be obtained in the intercalation compounds, the Rietveld refinement is valuable. For the hydrocarbon superconductors, however, the

Rietveld refinements have never been achieved because of its low crystal symmetry where the doped metal atoms do not occupy special symmetric sites unlike in the doped C_{60} compounds.

On the other hand, Raman scattering is known to be a powerful tool for determining the x value in A_xC_{60} .¹⁷⁻¹⁹ The A_g peak, which is observed at 1469 cm^{-1} for pure C_{60} (with I_h symmetry), shifts to lower frequencies when alkaline metal atoms are doped into C_{60} solids. Actually, the peak shifts by $6 - 7\text{ cm}^{-1}$ for one electron donation to a C_{60} molecule, namely, the A_g peak is observed at 1452 cm^{-1} for K_3C_{60} ,¹⁷ 1448 cm^{-1} for Rb_3C_{60} ¹⁸ and 1447 cm^{-1} for Cs_3C_{60} ,¹⁹ providing a good probe for determining the amount of doping. If we now turn to hydrocarbon systems, we previously suggested that some of the peaks shift to lower frequencies with increasing the x value in $K_x\text{picene}$ ² in a similar manner as in A_xC_{60} ,¹⁷⁻¹⁹ which indicates that the number of electrons on picene can be determined from the shift of Raman peaks from that of pure picene. The number of electrons on phenanthrene molecule in $A_x\text{phenanthrene}$ was successfully determined from the Raman spectrum, which indicates that the superconducting component is $A_3\text{phenanthrene}$. Thus three electron donation seems to be a key for superconductivity,³⁻⁵ but we have definitely to elaborate this. So the first purpose of the present study is to systematically investigate the Raman scattering for $A_x\text{picene}$ (A : K and Rb) to correlate the number of electrons on the hydrocarbon molecules with the Raman frequency. The experimental Raman frequencies have been measured for a wide range of $x = 0 - 5$ in $A_x\text{picene}$, which is compared with theoretical frequencies for the Raman peaks. From this, we have evaluated the number of electrons per picene molecule (or number of alkaline metal atoms) to clearly determine the number of x in superconducting phases.

Now, in characterizing physical properties of picene superconductors, it is intriguing to compare the picene superconductors with more familiar carbon-based superconductors, *i.e.*, C_{60} and graphite compounds intercalated with alkaline or alkaline earth metal atoms, where the highest T_c is 33 K for $RbCs_2C_{60}$ among C_{60} compounds,²⁰ and 11.5 K for CaC_6 among graphite compounds.²¹ One probe of these materials is the pressure dependence of T_c : indeed, C_{60} and graphite superconductors

have opposite tendencies; K_3C_{60} ($T_c = 18$ K) shows a large negative pressure coefficient ($dT_c/dP = -7.8$ K GPa⁻¹),²² while CaC_6 has a positive one ($dT_c/dP = 0.42 - 0.48$ K GPa⁻¹).²³ In the previous paper, we reported briefly the pressure dependence of T_c in 7 K phase of K_3 picene,² but the detailed analysis and data were not shown. Very recently, positive pressure dependence of T_c in A_x phenanthrene, AE_x phenanthrene and Ln_x phenanthrene was reported,³⁻⁵ which cannot be understood with a simple phonon mechanism of BCS superconductivity. Therefore it is interesting to examine the pressure dependence of T_c in the $T_c = 7$ and 18 K phases of picene superconductors, which may turn out to be an important key for investigating the mechanism of superconductivity. Thus the second purpose of the present paper is to explore the pressure dependence of 7 and 18 K phases of K_3 picene, here reported in a pressure region of 1 bar to 1.2 GPa. The pressure dependence is discussed from the viewpoints of crystal and electronic structures of picene superconductors.

The third purpose of the present paper is on the fabrication method for K_3 picene samples. A still unclear question is why we have two phases with $T_c = 7$ and 18 K. The usual annealing method (or solid-reaction method) does not allow us to produce selectively 7 or 18 K phases. Even a precise control of nominal composition in K_x picene from $x = 2.6$ to 3.3 produced both 7 K and 18 K superconductors.^{1,2} Here we have tried to prepare K_3 picene superconductor by a solution process with monomethylamine, CH_3NH_2 , as a solvent, in search for a synthetic method for selectively preparing 7 K or 18 K phase. The solution process has previously been used to control polymorphs of Cs_3C_{60} , which is a pressure-induced superconductor ($T_c = 38$ K (A15 phase) and $T_c = 35$ K (face-centered cubic phase) at 15 kbar).^{24,25} Here we show that the solution process with CH_3NH_2 for K_3 picene enables us to prepare selectively the K_3 picene sample exhibiting only $T_c = 18$ K.

II. Experimental

Picene (purity: 99.9%) was purchased from NARD Co Ltd., which was used for the experiments without further purification. Alkaline or alkaline earth metal was mixed with picene powder at nominal x value in a pyrex glass tube to fabricate

A_x picene. In the annealing method, the pyrex glass tube was pumped and sealed at 10^{-5} Torr. The tubes were annealed at temperatures as high as ~ 443 K for ~ 10 days. The samples obtained after annealing were black in color. The Raman spectrum and magnetic susceptibility were measured for the samples treated in a glove box without any exposure to air. The Raman scattering was measured at 295 K with Raman spectrometer (JASCO NRS-3100) with an excitation energy having a wavelength $\lambda = 785$ nm, while magnetization, M , was measured using a SQUID magnetometer (Quantum Design MPMS2) in the temperature region > 2 K under ambient and high pressures. A magnetic field, H , of 20 Oe was applied in measuring M/H . For the measurement of pressure dependence of superconductivity, a Cu-Be piston-cylinder type pressure-cell was used. The hydrostatic pressure was mediated by Daphne oil. The applied pressure region was from 1 bar to 1.2 GPa. A small piece of crystalline Sn or Pb was put inside the pressure cell along with the sample to monitor the exact pressure.

In the solution method for preparing A_x picene, on the other hand, CH_3NH_2 was introduced from the CH_3NH_2 gas bottle into the glass vessel containing picene powder and K metal at nominal stoichiometric amounts. The picene and K were completely dissolved in CH_3NH_2 by stirring at 223 K for 3 h. The color of solution was dark-green. After complete dissolution, liquid CH_3NH_2 was removed at 300 K until the base pressure reaches 10^{-4} Torr. The black powder sample obtained after removing CH_3NH_2 was moved into quartz tube in Ar filled glove box. The tube was dynamically pumped and sealed at 10^{-6} Torr. The tube was annealed at 443 K for 70 h to remove CH_3NH_2 completely. Special care was taken in the annealing procedure because high temperature annealing above 490 K for removal of CH_3NH_2 produces a very toxic material, KCN; actually even below 490 K, KCN may be produced. Powder X-ray diffractions for K_x picene were measured by RIGAKU RINT-TTR III in synchrotron radiation (KEK, PF and ESRF). The unit-cell parameters for K_x picene were determined by the LeBail analysis program in GSAS package.²⁶ Theoretical calculation of Raman frequencies and intensities for A_1 , A_2 , B_1 and B_2 modes for neutral picene and its anions, picene^{y-} ($y = 0 - 5$), with optimized structure (C_{2v} symmetry) was performed with B3LYP program based on hybrid Hartree-Fock (HF)

/ density functional theory (DFT) with the 6-31G* basis set.²⁷⁻²⁹

III. Results and Discussions

III-1. Characterization of the number of doped metal atoms in K_x picene and Rb_x picene

Figures 1(a) and 2(a) show Raman spectra for samples of K_x picene and Rb_x picene ($x = 0 - 5$), respectively, at $500 - 1800 \text{ cm}^{-1}$. A pronounced peak at 1378 cm^{-1} marked with an asterisk can be assigned to superposition of ν_{20} and ν_{21} A_1 vibration modes of picene molecule, where ν_{19} , ν_{20} and ν_{21} stand for the 19th, 20th and 21st A_1 vibration modes from the lowest mode, respectively. The ν_{20} and ν_{21} modes in picene^{y-} ($y = 0 - 5$) are schematically depicted in Fig. 3. These vibration modes are suggested to provide strong electron-phonon coupling.⁸ In Figs. 1(b) and 2(b) the theoretical frequencies and intensities of Raman active A_1 , A_2 , B_1 and B_2 vibration modes are shown along with the experimental Raman spectra, and the experimental peaks are seen to agree well with the theoretical results. Figs. 1 and 2 also show that the pronounced peak observed at 1378 cm^{-1} for neutral picene shifts to lower frequencies with an increase in x for both K_x picene and Rb_x picene samples.

The average values of ν_{20} and ν_{21} calculated theoretically are plotted for each picene molecule in Figs. 4(a) and (b). The experimental frequencies for the pronounced peak, which are ascribable to superposition of ν_{20} and ν_{21} for K_x picene and Rb_x picene, are plotted as a function of x in Figs. 4(a) and (b), respectively. As seen from Fig. 4(a), the experimental frequencies in all the K_x picene samples basically fall upon three discrete values, 1378 , 1344 and 1313 cm^{-1} , which are consistent with those predicted theoretically for picene, picene²⁻ and picene³⁻ (respective dashed lines). This implies that, aside from the pristine picene, only two phases, K_2 picene and K_3 picene, can be produced in K_x picene samples. As for K_1 picene sample, this separates into two phases, picene and K_2 picene, as seen from Figs. 1(b) and 4(a). The same plots suggest that $K_{1.5}$ picene and K_2 picene samples decompose into three phases of picene, K_2 picene and K_3 picene.

Further, the Raman peak in K_x picene samples was observed at 1328 cm^{-1} in addition to those for K_2 picene (at 1344 cm^{-1}) and K_3 picene (1313 cm^{-1}), where the value (1328 cm^{-1}) is intermediate between 1344 cm^{-1} and 1313 cm^{-1} . The Raman peak at 1328 cm^{-1} implies the existence of phase with a fractional x ($K_{2.5}$ picene), although the phase is not a main one. However, two Raman peaks should be observed at 1344 and 1313 cm^{-1} because Raman scattering reflects vibration of molecule even if the $K_{2.5}$ picene phase appears as statistically averaged structure in this sample. Thus the origin of the Raman peak at 1328 cm^{-1} remains to be clarified. If a dynamic conversion of picene²⁻ and picene³⁻ produces the peak at 1328 cm^{-1} , the Raman scattering should be observed at low temperatures with the single peak splitting to peaks at 1344 and 1313 cm^{-1} . When nominal x value was increased above 3, only K_2 picene and K_3 picene were observed, while K_4 picene and K_5 picene phases could not be fabricated, which indicates that the maximum x value is three. From these plots, we conclude that only two phases, K_2 picene and K_3 picene, can be realized by an intercalation of K atoms into picene samples, while K_1 picene is unstable. In Fig. 4(a), the plot for phases with the same x value as the nominal x in the K_x picene sample is indicated in red (e.g., the Raman peak assigned to K_3 picene phase in the K_3 picene sample).

Here, we should stress that the prepared individual K_x picene sample does not always contain all the crystal phases described above, but that some solid samples contain only one or two crystal phases. The number of the phases appearing in each sample is given in parentheses in Fig. 4(a). The numbers then indicate the frequency with which the crystal phases appear. For example, all K_3 picene samples (19 pieces) contained the K_3 picene crystal-phase, and 58% in 19 pieces of K_3 picene samples showed only a peak ascribable to K_3 picene crystal phase *i.e.*, a single phase of K_3 picene, while K_2 picene samples produce either a single phase of K_2 picene (25%) or picene/ K_2 picene/ K_3 picene phases (25%). Other K_2 picene samples provided a single phase of K_3 picene (25%) or K_2 picene/ K_3 picene (25%). K_1 picene samples resulted in a single phase of K_2 picene (33%) or picene/ K_2 picene phases (66%). $K_{1.5}$ picene samples provided picene/ K_2 picene phases (25%) or picene/ K_2 picene/ K_3 picene phases (50%) in which each fraction of phase (peak

intensity) was almost the same. The $K_{1.5}$ picene samples provided only a single phase of K_2 picene (25%). It is suggested from these results that K metal in solid picene may not completely react in most of the samples except for samples producing a single phase. Judging from the probability, 58%, of realization of single phase, it is suggested that K_3 picene is more stable phase than K_2 picene (25% for a single phase). Therefore, it is of interest to investigate theoretically the energetic stability of K_x picene phase.

As seen from Figs. 2(b) and 4(b), the frequencies of ν_{20} , ν_{21} Raman peaks in Rb_x picene samples also suggest existence of only three phases (picene, Rb_2 picene and Rb_3 picene) as in K_x picene. The observed frequencies, 1378, 1345 and 1313 cm^{-1} , can be assigned to picene, picene^{2-} and picene^{3-} , respectively; the values are consistent with those of K_x picene. It can be concluded from the plots (Fig. 4(b)) that Rb_1 picene sample provides only two phases, picene and Rb_2 picene, while Rb_2 picene and Rb_3 picene solid samples provide only three phases (picene, Rb_2 picene and Rb_3 picene). Thus, increasing nominal x leads to a realization of phases with larger x , in the same manner as in K_x picene (Fig. 4(a)). Increasing nominal x above 3 produces Rb_3 picene and picene as well as a new phase of $Rb_{2.5}$ picene exhibiting the Raman frequency of 1323 cm^{-1} , whose phase was also found in K_x picene. In the same manner as K_x picene, the stability of Rb_3 picene is confirmed because of high probability, 44%, of formation of a single phase in the Rb_3 picene samples.

The magnetic susceptibility has been measured for all the samples of K_x picene and Rb_x picene. The $M/H - T$ curves for K_x picene samples showing the existence of K_3 picene phase (with the Raman peak at $\sim 1313 \text{ cm}^{-1}$) exhibits a clear drop at 7 or 18 K, indicating the superconducting transition. Conversely, all the samples that have no K_3 picene phase do not show such a behavior. These results clearly show that superconducting phase in K_x picene relates closely to K_3 picene phase. The M/H of Rb_x picene samples also show the same behavior, *i.e.*, the samples showing the existence of Rb_3 picene phase have the superconducting transition, while the Rb_3 picene samples that do not exhibit the Raman peak at $\sim 1313 \text{ cm}^{-1}$ exhibit no superconducting transition, indicating that superconducting phase relates to Rb_3 picene. Thus, we have identified that superconducting phases in K_x picene and

Rb_xpicene can be closely associated with K₃picene and Rb₃picene crystal phases, respectively, from the M/H and Raman scattering.

III-2. Pressure dependence of superconducting transition temperature in 7 K and 18 K phases

The $M/H - T$ curves at various pressures are displayed for the 7 K superconducting phase (K₃picene) which shows that the T_c shifts downward with pressure, but only gradually. The pressure dependence of the midpoint of the superconducting transition, T_c^{mid} , is shown in Fig. 5b. The T_c^{mid} decreases linearly with pressure up to 1 GPa, with $dT_c^{\text{mid}}/dP = -0.3 \text{ K GPa}^{-1}$, which can be determined unambiguously because of the absence of any inhomogeneous broadening of the superconductive transition with increasing pressure. So dT_c/dP of the 7 K phase has the same negative sign as that of K₃C₆₀, but is an order of magnitude smaller. K₃C₆₀ has a three-dimensional (3D) electronic band structure, and pressure is expected to increase the bandwidth, which will cause a decreased density of states (DOS) at the Fermi energy, $N(\epsilon_F)$,²² which in turn decreases T_c , regardless of a softening of some C₆₀ vibration modes.³⁰ The intercalated graphite, CaC₆, on the other hand, has a positive pressure dependence, where the electronic structure around the Fermi energy is shown to contain a large component of the so-called interlayer states, whose amplitudes reside in between the graphene layers, conferring a 3D character on the electronic structure.^{23,31} In this compound, while the $N(\epsilon_F)$ decreases with pressure, a large softening of an in-plane Ca vibration mode under pressure is shown to cause an increase in the electron-phonon coupling λ , which is considered to overcome the reduction of $N(\epsilon_F)$, leading to an enhanced T_c .

In K₃picene, the electronic structure calculation¹⁰ indicates that the interlayer band lies well above the Fermi energy, while the character of the conduction band primarily originates in the LUMO/LUMO+1 orbitals of the picene molecule. More importantly, the wave functions in the conduction band have large amplitudes on the doped K atoms, so that the dopants act not only as a source of charge transfer, but cause a strong hybridization with the aromatic system. We can thus argue that the

small reduction of T_c against pressure in K_3 picene may be related to the structure of the conduction bands arising from the strongly-coupled molecules and dopants.

As reported previously,² when the x value in K_x picene and Rb_x picene is increased, the a -axis is expanded while the b - and c -axes are shrunk, leading to the reduction of unit-cell volume. This implies that the picene molecules become more densely packed when doped with K. This peculiarity comes from a deformation of the in-layer, herringbone arrangement of picene molecules.^{1,2} A theoretical structure optimization¹⁰ indeed indicates that the angle between picene molecules in the herringbone arrangement changes dramatically from 61° to 114° as the metal atoms are inserted in the layer. These are further indications that the picene molecules and metal atoms form a strongly-knit layer, which is consistent with the small pressure dependence of T_c . Furthermore, T_c in the 7 K phase of A_3 picene is similar for $A = K$ and Rb ,¹ unlike in fulleride superconductors,³² *i.e.*, the chemical-pressure effect is rather small in the aromatic compounds. To summarize, the 7 K superconducting phase is robust against both physical and chemical pressures.

Now we turn to the pressure dependence of T_c in the 18 K phase of K_3 picene. Figure 6(a) shows the M/H against T , normalized by the value at 50 K for clarity, for various pressures in the 18 K superconducting phase. We can immediately notice that the superconducting onset temperature, T_c^{onset} , shifts *upward*. The T_c^{onset} , shown in Fig. 5(b) against pressure, increases linearly with pressure up to 1.2 GPa, with $dT_c^{\text{onset}}/dP = 12.5 \text{ K GPa}^{-1}$. The large positive pressure dependence found here contrasts sharply with the negative pressure dependence in the 7 K phase. The positive pressure dependence has also observed in A_3 phenanthrene, $AE_{1.5}$ phenanthrene and Ln_1 phenanthrene.³⁻⁵ However, the size of the coefficient, dT_c^{onset}/dP , is an order of magnitude larger than that, $\sim 1 \text{ K GPa}^{-1}$, of phenanthrene superconductor. Since a reduced volume usually implies a smaller DOS at ϵ_F , this behavior cannot be understood with a simple phonon mechanism of BCS superconductivity.

III-3. Selective preparation of 18 K superconducting phase in K_3 picene

For $K_{3.1}$ picene sample (nominal $x = 3.1$) that was prepared by the solution process, Fig. 7(a) shows the $M/H - T$ curve in zero-field cooling (ZFC). This data was reported and briefly discussed in ref. 2. Before annealing the sample or removing CH_3NH_2 from the precursor, the M/H shows a Pauli-like, temperature-independent behavior with a weak increase below 10 K. After the sample is annealed at 443 K for 70 h, the M/H begins to show an abrupt decrease with the $T_c^{\text{onset}} = 18$ K and the $T_c^{\text{mid}} = 17$ K. This superconducting transition coincides with that for the 18 K phase of K_3 picene superconductor prepared by solid-reaction method, or annealing method.^{1,2} The maximum shielding fraction is still as low as 0.1%, a value lower by an order of magnitude than that, 1.2 %, for 18 K superconductor prepared by annealing method.¹ However, we notice that the solution-reaction method can produce 18 K superconducting phase more effectively than by solid-state method. In fact all the K_3 picene samples prepared by solution method show a clear decrease in M/H at 18 K. The nominal x value for producing the superconducting phase by solution process is confined to 2.9 – 3.1, suggesting that three K atoms are doped per picene molecule.

Figure 7(b) shows Raman scattering spectra for the K_3 picene samples prepared by the solution method. One sample (top curve in Fig. 7(b)) was annealed at 443 K for 70 K in vacuum to remove CH_3NH_2 , while the other (the second curve) was not annealed. For comparison, the spectra for the K_3 picene sample (the second from the bottom) prepared by the solid-reaction method as well as for pristine picene (bottom) are also shown. We can see that the Raman spectrum for the $K_{3.1}$ picene sample (top: solution method) coincides with that for the $K_{3.0}$ picene (the second from the bottom: solid-reaction method), where the peak shifts to a lower frequency by 67 cm^{-1} from that, 1378 cm^{-1} , for pristine picene, showing that these samples possess the same number of electrons for a picene molecule, *i.e.*, these can be represented as K_3 picene. This result indicates the effectiveness of annealing at 443 K in vacuum for the removal of CH_3NH_2 , and it may be recognized that CH_3NH_2 molecules are scarcely left in $K_{3.1}$ picene sample (top curve in Fig. 7(b)). On the other hand, the peak for the $(CH_3NH_2)K_{3.0}$ picene sample (the third from the bottom in Fig. 7(b)), which was prepared by solution method and was not annealed, shifts

to a lower frequency by 48 cm^{-1} , showing that 2.5 electrons are transferred to picene molecule from K atoms. This implies that the remaining CH_3NH_2 molecule may capture 0.5 electrons from a picene molecule, *i.e.*, a back-electron transfer from picene molecule.

Figures 8(a) and (b) show the X-ray diffraction patterns for the $(\text{CH}_3\text{NH}_2)_2\text{K}_3\text{picene}$ and K_3picene samples, respectively. The former sample was prepared by the solution method without any annealing. The latter was prepared by the solution method with annealing at 443 K for 70 h. The lattice parameters for two samples obtained from the LeBail fit to X-ray diffraction patterns (Fig. 8) are listed in table 1; the space group was assumed to be $P2_1$ in these samples, in the same manner as picene and K_3picene prepared by solid reaction method.^{1,2} We can see from this table that the lattice parameters, a and c , for the K_3picene sample prepared by the solution method without annealing increase in comparison with those in picene. Specifically, the c axis expands markedly, suggesting that CH_3NH_2 molecules are mainly intercalated into the space between the herringbone layers of picene molecules (ab -layers).

Actually, the values of a and c in the K_3picene sample, prepared by the solution method with annealing, are smaller than those in the sample without annealing, showing that CH_3NH_2 was basically removed in the sample annealed at 443 K under vacuum, which is consistent with the results obtained from the Raman scattering. The K_3picene sample prepared by the solid reaction (the second from the bottom in Fig. 7(b)) showed T_c of 7 K, while the K_3picene sample (top curve in Fig. 7(b)), prepared by the solution method with annealing, showed T_c of 18 K. All the lattice parameters in the K_3picene sample prepared by the solution method with annealing are larger than those in pure picene, especially the c expands, suggesting that the crystal structure of K_3picene phase prepared by solution method is different from that (7 K phase) prepared by the solid reaction, *i.e.*, the K atoms in K_3picene prepared by the solution method may be intercalated into the space between ab -layers.

In fact, the theoretical calculation (as summarized in table 2 for the structure parameters^{10,33,34}) shows existence of two kinds of doping structures: (i) the one (denoted as K_3picene) with the dopants inserted within the herringbone-arranged picene layer (ab -layer), and (ii) another with some dopants intercalated in the

interlayer regions as well, where the latter is meta-stable but does exhibit a local energy minimum. The structure is denoted as K_2K_1 picene where two K atoms are inserted into the *ab*-layer while one K atom is intercalated into the space between *ab*-layers.^{2,10} The lattice constants determined by X-ray diffraction indicate the expansion of *a*-axis and shrinkage of *c*-axis in the 7 K phase prepared by solid reaction, suggesting the intercalation of K atoms into the picene layer (*ab*-layer), which is consistent with the location of K atoms with intralayer insertion obtained theoretically.¹⁰ On the other hand, some of the K atoms in K_3 picene prepared by solution method may be intercalated into the space between *ab*-layers, which is consistent with the theoretical prediction that the structure with both intralayer and interlayer dopants is a meta-stable structure.^{10,33,34} Thus the theoretical structure may possibly be related to the 18 K phase prepared by solution method, but this definitely requires further confirmation.

As for the superconducting mechanism and the symmetry of the gap function has yet to be understood. The previous theoretical calculation suggests that the electron-phonon coupling is sufficiently strong to roughly account the size of T_c in doped picene.^{8,9,35} At the same time, the possible relevance of the strong electron-electron correlation is pointed out in the other theoretical works.³⁶⁻³⁸ The multiple structures, found here to be dependent on the sample fabrication method, is consistent with the previous theoretical suggestion that there are multiple meta-stable structures in the doped picene.^{10,33,34} More importantly, if the identification of the 18 K phase of the superconductivity to be the structure with the intralayer plus interlayer insertion of dopants is correct, this implies the superconductivity is dominated by details in the doping structure, and this may give a crucial clue in exploring the superconductivity mechanism, including some unconventional ones. Indeed, here we find that the samples with the 7 K phase and the 18 K phase react in opposite manners against the applied pressure, which may provide an important test in sorting the mechanism. The first thing we should check theoretically is how the DOS changes against pressure. As shown theoretically^{10,33,34}, the conduction band comprises multiple orbitals, so that the DOS may show a nontrivial dependence on the pressure. The next interest is how the shape of the Fermi surface, which can be crucial in unconventional superconductivity, changes against pressure. This is

interesting, since even at ambient pressure the Fermi surface is shown to be a composite of pieces with different dimensionalities^{10,33,34}. Such a study is under way, and will be reported elsewhere.

IV. Conclusion

The conclusion of the present paper is three-fold: (i) We have performed a characterization of the number of electrons on picene molecule by use of Raman scattering, and the two different phases of A₂picene and A₃picene were found in the A_xpicene samples, indicating the absence of A₁picene phase. From the Raman scattering of superconducting A_xpicene samples, it has been found that the A₃picene phase relates closely to superconducting phase. (ii) The pressure study revealed that the 18 K phase has a positive dT_c^{mid}/dP as in superconducting phenanthrene³⁻⁵, while the 7 K phase has a negative coefficient. The latter is understandable from the BCS picture, while the former does not fit with a simple phonon-mechanism BCS superconductivity. (iii) The preparation of K₃picene by a solution method led selectively to 18 K superconducting phase, which is different from the preparation by annealing method which produces 7 or 18 K phase. The K₃picene sample prepared by the solution method showed longer *c* axis than in K₃picene by the annealing method, indicating that the K atoms may be intercalated into the space between the herringbone (*ab*) layers. Thus, this study shows a new synthesis method for production of crystal phase (K₃picene) exhibiting only an 18 K superconducting transition and characterizes the crystal phase.

Acknowledgment. The authors appreciate to Prof. Masasaki Mifune of Department of Pharmaceutical Science, Okayama University, for his valuable assistance in the Raman measurement. HA is benefitted from discussions with Taichi Kosugi of AIST. This study is partly supported by Grant-in-aid (23340104, 23684028, 22244045, 24654105) of MEXT, by the LEMSUPER project (JST-EU Superconductor Project) in Japan Science and Technology Agency (JST), and by Special Project of Okayama University / MEXT. The X-ray diffractions with synchrotron radiation were done under the proposals of KEK-PF (2011G109), SPring-8 (2011A1938) and ESRF (HS-4556).

References

1. R. Mitsuhashi, Y. Suzuki, Y. Yamanari, H. Mitamura, T. Kambe, N. Ikeda, H. Okamoto, A. Fujiwara, M. Yamaji, N. Kawasaki, Y. Maniwa, Y. Kubozono, *Nature* 464, 76 (2010).
2. Y. Kubozono, H. Mitamura, X. Lee, X. He, Y. Yamanari, Y. takahashi, Y. Suzuki, Y. Kaji, R. Eguchi, K. Akaike, T. Kambe, H. Okamoto, A. Fujiwara, T. kato, T. Kosugi, H. Aoki, *Phys. Chem. Chem. Phys.* 13, 16476 (2011).
3. X. F. Wang, R. H. Liu, Z. Gui, Y. L. Xie, Y. J. Yan, J. J. Ying, X. G. Luo, X. H. Chen, *Nature Commun.* 2, 507 (2011).
4. X. F. Wang, Y. J. Yan, Z. Gui, R. H. Liu, J. J. Ying, X. G. Luo, X. H. Chen. *Phys. Rev. B.* 84, 214523 (2011).
5. X. F. Wang, X. G. Luo, J. J. Ying, Z. J. Xiang, S. L. Zhang, R. R. Zhang, Y. H. Zhang, Y. J. Yan, A. F. Wang, P. Cheng, G. J. Ye, X. H. Chen, *J.Phys.:Condens. Matter*, 24, 345701(2012).
6. M. Xue, T. Cao, D. Wang, Y. Wu, H. Yang, X. Dong, J. He, F. Li, G. F. Chen, *Scientific Reports*, 2, 389; DOI: 10.1038/srep00389 (2012).
7. J. E. Schirber, D. L. Overmyer, K. D. Carlson, J. M. Williams, A. M. Kini, H. Hau Wang, H. A. Charlier, B. J. Love, D. M. Watkins, and G. A. Yaconi, *Phys. Rev. B* 44, 4666 (1991).
8. T. Kato, T. Kambe, Y. Kubozono, *Phys. Rev. Lett.*, 107, 077001 (2011).
9. M. Casula, M. Calandra, G. Profeta, F. Mauri, *Phys. Rev. Lett.* 107, 137006 (2011).
10. T. Kosugi, T. Miyake, S. Ishibashi, R. Arita, H. Aoki, *J. Phys. Soc. Jpn.* 78, 113704 (2009).
11. H. Okazaki, T. Wakita, T. Muro, Y. Kaji, X. Lee, H. Mitamura, N. Kawasaki, Y. Kubozono, Y. Yamanari, T. Kambe, T. Kato, M. Hierai, Y. Muraoka, *Phys. Rev. B*, 82,195114 (2010).
12. J. Ying, X. Wang, Y. Yang, Z. Xiang, X. Luo, Z. Sun, X. Chen, *Phys. Rev. B* 85, 180511(R) (2012).
13. Y. Kasahara, Y. Takeuchi, Y. Iwasa, *Phys. Rev. B* 85, 214520 (2012).
14. P. W. Stephens, L. Mihaly, P. L. Lee, R. L. Whetten, S.-M. Huang, R. Kaner, F.

- Deiderich, K. Holczer, *Nature*, 351, 632 (1991).
15. O. Zhou, D. E. Cox, *J. Phys. Chem. Solids* 53, 1373 (1992).
 16. C. A. Christine, G. M. Bendele, P. W. Stephens, *Phys. Rev. B* 55, R3366 (1997).
 17. T. Pichler, M. Matus, J. Kürti, H. Kuzmany, *Phys. Rev. B* 45, R13841 (1992).
 18. M. S. Dressellhaus, G. Dressellhaus, and P. C. Eklund, *J. Raman Spectros.* 27, 351 (1996), and references therein.
 19. S. Fujiki, Y. Kubozono, S. Emura, Y. Takabayashi, S. Kashino, A. Fujiwara, K. Ishii, H. Suematsu, Y. Murakami, Y. Iwasa, T. Mitani, H. Ogara, *Phys. Rev. B* 62, 5366 (2000).
 20. K. Tanigaki, T. W. Ebbesen, S. Saito, J. Mizuki, J. S. Tsai, Y. Kubo, S. Kuroshima, *Nature*, 352, 222 (1991).
 21. N. Emery, C. Hérold, M. d'Astuto, V. Garcia, Ch. Bellin, J. F. Marêche, P. Lagrange, G. Loupiau, *Phys. Rev. Lett.*, 95, 087003 (2005).
 22. G. Sparr, J. D. Thompson, S.-M. Huang, R. B. Kaner, F. Diederich, R. L. Whetten, G. Grüner, K. Holczer, *Science*, 252, 1829 (1991).
 23. J. S. Kim, L. Boeri, R. K. Kremer, F. S. Razavi, *Phys. Rev. B* 74, 214513 (2006).
 24. A. Y. Ganin, Y. Takabayashi, Y. Z. Khimyak, S. Margadonna, A. Tamai, M. J. Rosseinsky, K. Prassides, *Nature Mater.* 7, 367 (2008).
 25. Y. Takabayashi, A. Y. Gannin, P. Jeglic, D. Arcon, T. Takano, Y. Iwasa, Y. Ohishi, M. Takata, N. Takeshita, K. Prassides, M. J. Rosseinsky, *Science*, 323, 1585 (2009).
 26. A.C. Larson and R.B. Von Dreele, "General Structure Analysis System (GSAS)", Los Alamos National Laboratory Report LAUR 86-748 (2000).
 27. A. D. Becke, *Phys. Rev. A* 38, 3098 (1988).
 28. C. Lee, W. Yang, R. G. Parr, *Phys. Rev. B* 37, 785 (1988).
 29. R. Ditchfield, W. J. Hehre, J. A. Pople, *J. Chem. Phys.* 54, 724 (1971).
 30. D. W. Snoke, Y. S. Raptis, K. Syassen, *Phys. Rev. B* 45, 14419 (1992).
 31. G. Csányi, P. B. Littlewood, A. H. Nevidomsky, C. J. Pickard, B. D. Simons, *Nature Phys.* 1, 42 (2005).
 32. R. M. Fleming, A. P. Ramirez, M. J. Rosseinsky, D. W. Murphy, R. C. Haddon, S. M. Zahurak, A. V. Makhija, *Nature* 352, 787 (1991).
 33. T. Kosugi, T. Miyake, S. Ishibashi, R. Arita, H. Aoki, *Phys. Rev. B* 84, 214506 (2011).

- 34. T. Kosugi, T. Miyake, S. Ishibashi, R. Arita and H. Aoki, Phys. Rev. B 84, 020507(R) (2011).
- 35. A. Subedi and L. Boeri, Phys. Rev. B 84, 020508(R) (2011).
- 36. G. Giovannetti and M. Capone, Phys. Rev. B 83, 134508 (2011).
- 37. M. Kim, B. I. Min, G. Lee, H. J. Kwon, Y. M. Rhee, and J. H. Shim, Phys. Rev. B 83, 214510 (2011).
- 38. Y. Nomura, K. Nakamura, and R. Arita, Phys. Rev. B 85, 155452 (2012).

Table 1. Experimentally obtained lattice parameters for picene and K-doped picene.

	a (Å)	b (Å)	c (Å)	β (°)	$V(\text{Å}^3)$
Picene ^{a)}	8.472(2)	6.170(2)	13.538(7)	90.81(4)	708
K ₃ picene ^{b)}	8.707(7)	5.912(4)	12.97(1)	92.77(5)	667
(CH ₃ NH ₂) _z K ₃ picene ^{c)}	8.927(5)	6.151(1)	14.476(4)	94.16(3)	793
K ₃ picene ^{d)}	8.571(5)	6.270(2)	14.001(3)	91.68(3)	752

a) Taken from ref. 1.

b) Taken from ref. 1, where the sample was prepared by solid reaction method.

c) Sample prepared by solution method without annealing.

d) Sample prepared by solution method with annealing.

Table 2. Theoretically obtained lattice parameters for K-doped picene.³³ K₃picene stands for a structure where all the three K atoms are inserted within the picene layer (with two possible structures A and B), while K₂K₁picene a structure with two intralayer atoms and one interlayer one.

	a (Å)	b (Å)	c (Å)	β (°)	$V(\text{Å}^3)$
K ₂ K ₁ picene	8.776	6.394	13.346	94.03	747.069
K ₃ picene (A)	7.421	7.213	14.028	104.53	726.848
K ₃ picene (B)	7.408	7.223	14.116	105.93	726.328

Figure captions

Fig. 1. Raman scattering spectra in K_x picene ($x = 0 - 5$) at (a) $500 - 1800 \text{ cm}^{-1}$ and (b) $1250 - 1400 \text{ cm}^{-1}$. Raman peaks calculated theoretically are indicated with bars in (b) with A_1 (B_2) mode in red (blue). The height of the red bars represents the relative intensities of the Raman peak. All the theoretical results are shifted downward by 27 cm^{-1} so that the theoretical average value of ν_{20} and ν_{21} A_1 modes in neutral picene fits to its experimental average value, 1378 cm^{-1} . The arrows indicate averaged values of theoretical ν_{20} and ν_{21} A_1 modes. The explanation of notation, ν_i , is described in text.

Fig. 2. A similar plot as in Fig.1 for Rb_x picene ($x = 0 - 5$).

Fig. 3. ν_{20} and ν_{21} A_1 modes schematically shown for picene^{y-} ($y = 0 - 5$).

Fig.4. Plots of frequency of experimental and theoretical Raman peaks against the nominal value, x , in (a) K_x picene and (b) Rb_x picene ($x = 0 - 5$). Frequency of the theoretical Raman peak corresponds to the average value of frequencies for ν_{20} and ν_{21} A_1 modes. The theoretical plots are shifted by 27 cm^{-1} so that the theoretical average value of ν_{20} and ν_{21} A_1 modes in neutral picene fits to its experimental average value, 1378 cm^{-1} . The experimental plots in red refer to the K_x picene (Rb_x picene) phase produced in the K_x picene (Rb_x picene) sample (see text). The numerical value in parenthesis stands for the number of times the phase appeared in each sample.

Fig. 5. (a) $M/H - T$ curves for various pressures, and (b) pressure dependence of T_c^{mid} in the 7 K superconducting phase of $K_{3.3}$ picene. dT_c^{mid}/dP is determined by a linear fitting in $T_c^{\text{mid}} - T$ plot.

Fig. 6. Similar plot as in Fig.5 for the 18 K superconducting phase of $K_{3.3}$ picene.

Fig. 7 (a) $M/H - T$ curve in zero-field cooling (ZFC) for $(\text{CH}_3\text{NH}_2)\text{K}_3\text{picene}$ and

$K_{3.1}$ picene samples, which were prepared by the solution process (see text). This data was reported and briefly discussed in ref. 2. (b) Raman scattering spectra for the K_3 picene samples which were prepared by the solution method (orange curve), $(CH_3NH_2)K_3$ picene (green), K_3 picene sample prepared by the solid-reaction method (blue), and pristine picene (black).

Fig. 8. X-ray diffraction patterns for (a) $(CH_3NH_2)K_3$ picene and (b) K_3 picene samples. Red circles (blue lines) show the observed (calculated) diffraction patterns. The green line shows the difference between the observed and calculated patterns. Black vertical bars correspond to the predicted peak positions. The lattice parameters for two samples, $(CH_3NH_2)K_3$ picene and K_3 picene, obtained from the Le Bail fit to X-ray diffraction patterns are listed in Table 1.

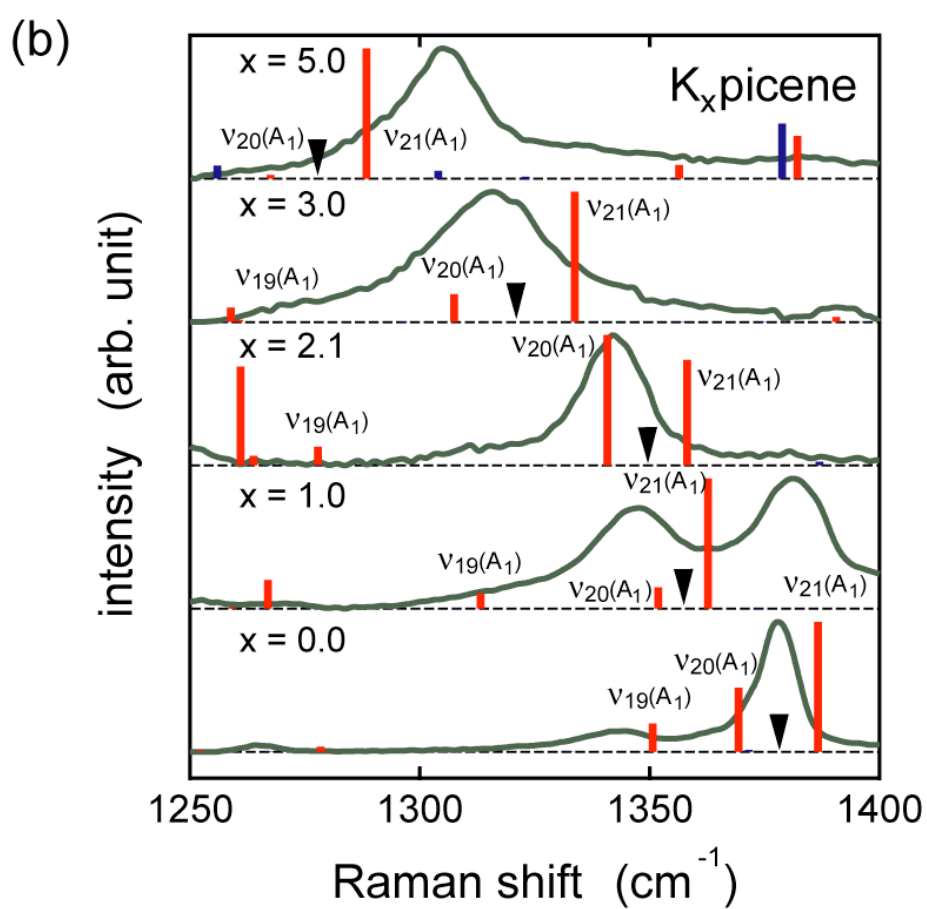
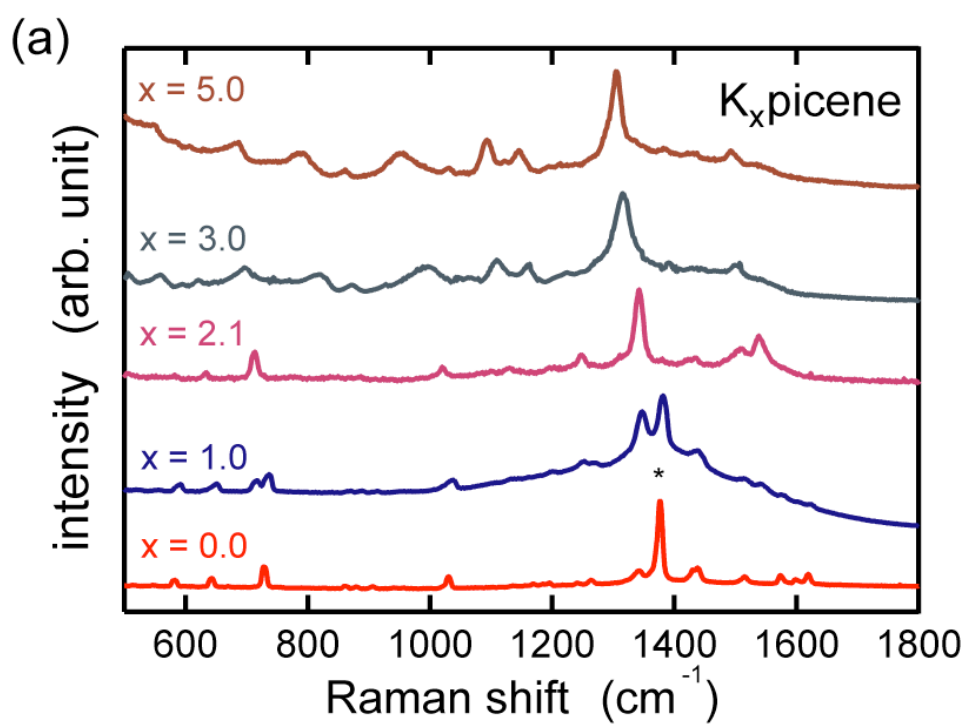


Figure 1. T. Kambe et al.,

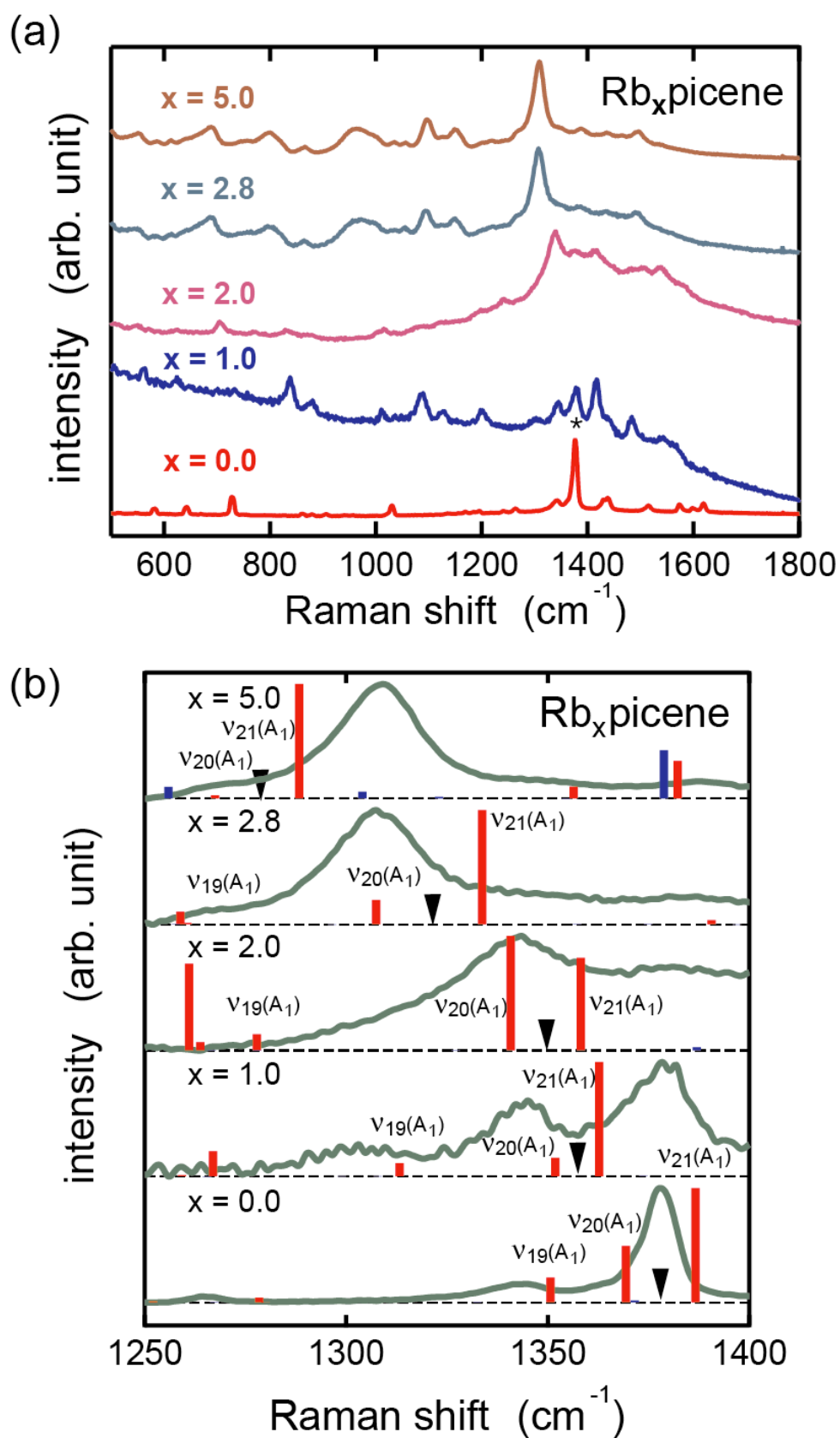


Figure 2. T. Kambe et al.,

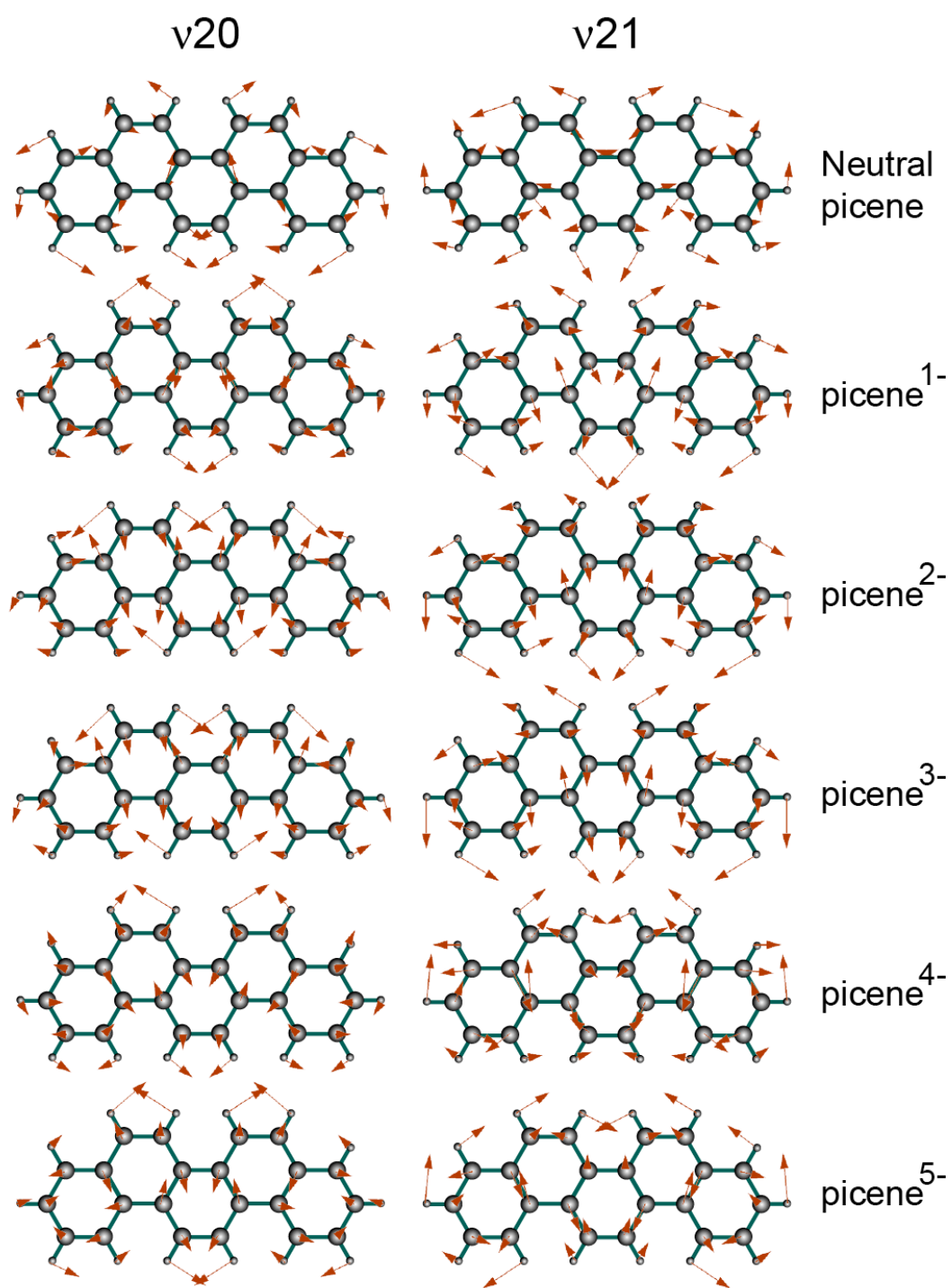
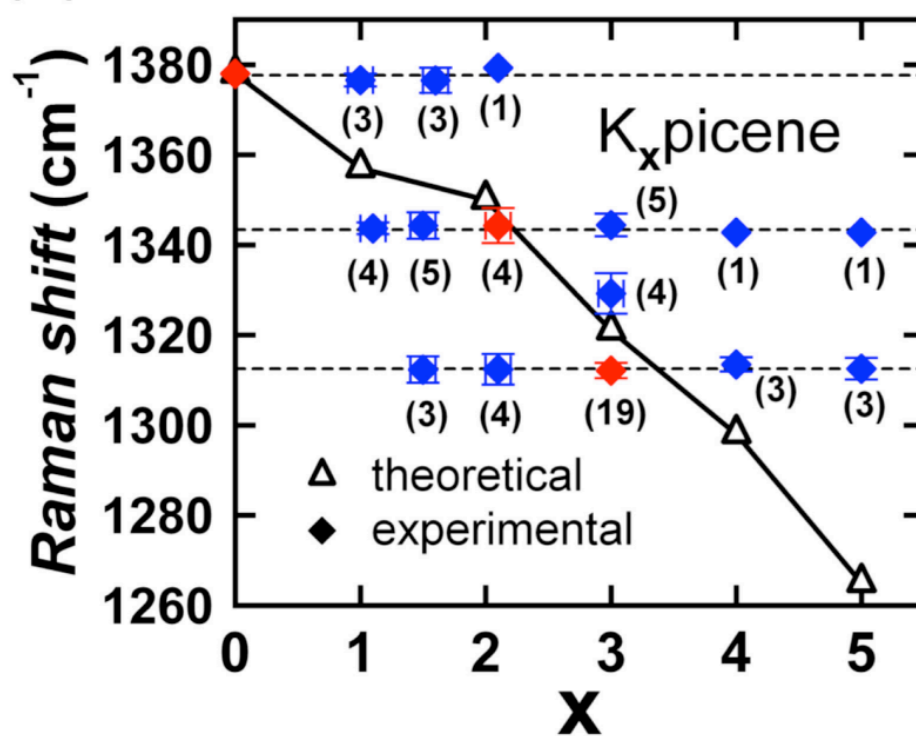


Figure 3. T. Kambe et al.,

(a)



(b)

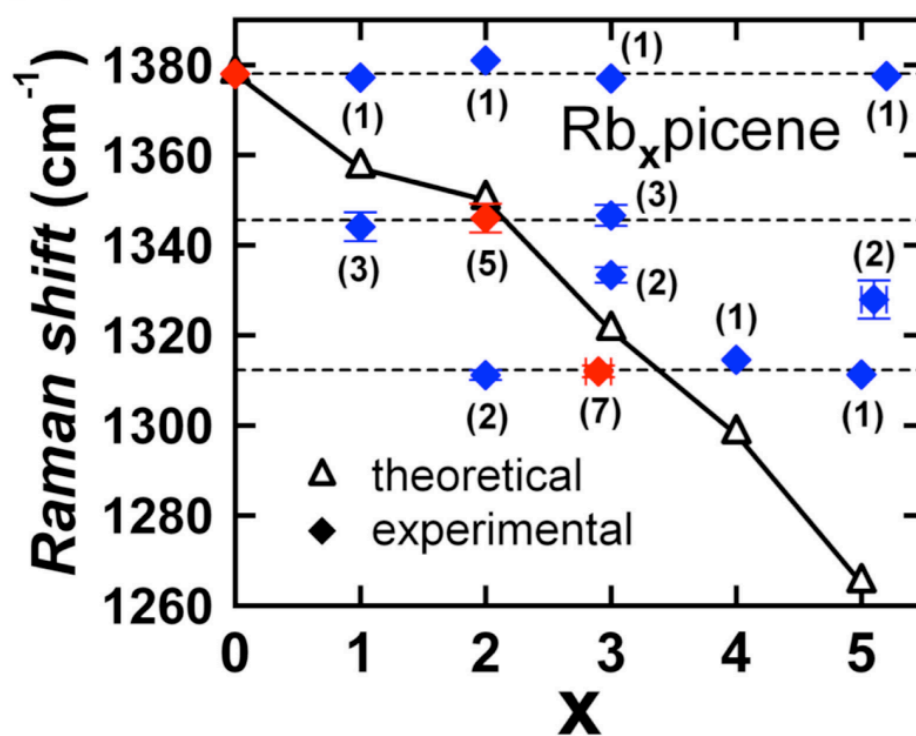


Figure 4. T. Kambe et al.,

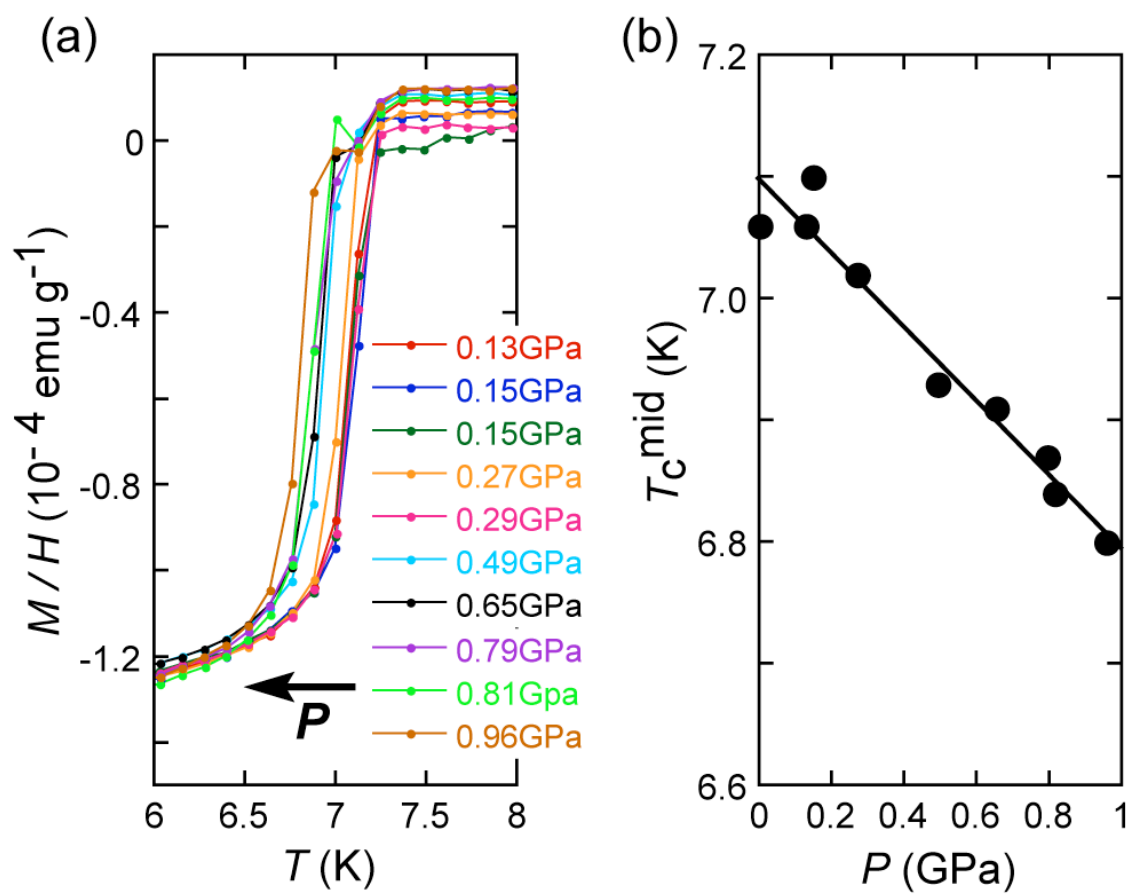


Figure 5. T. Kambe et al.,

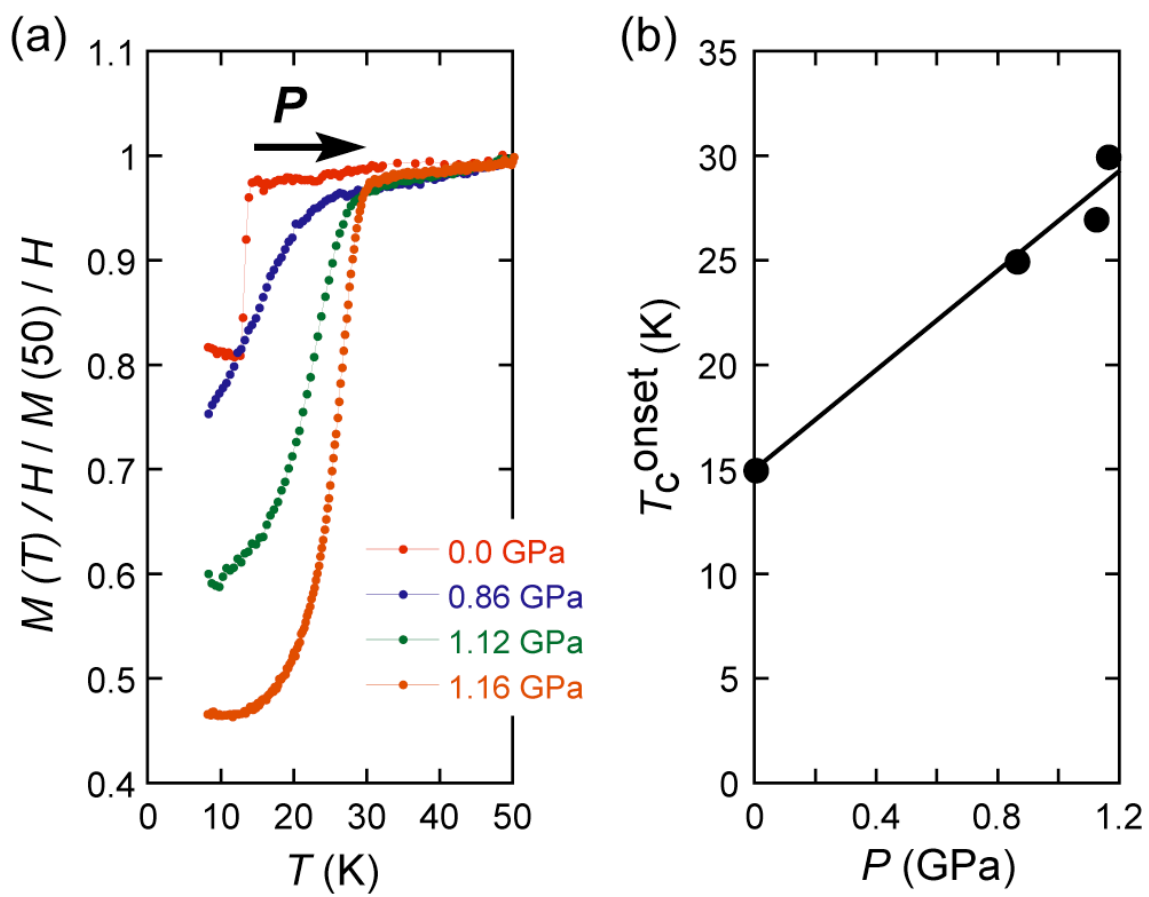


Figure 6. T. Kambe et al.,

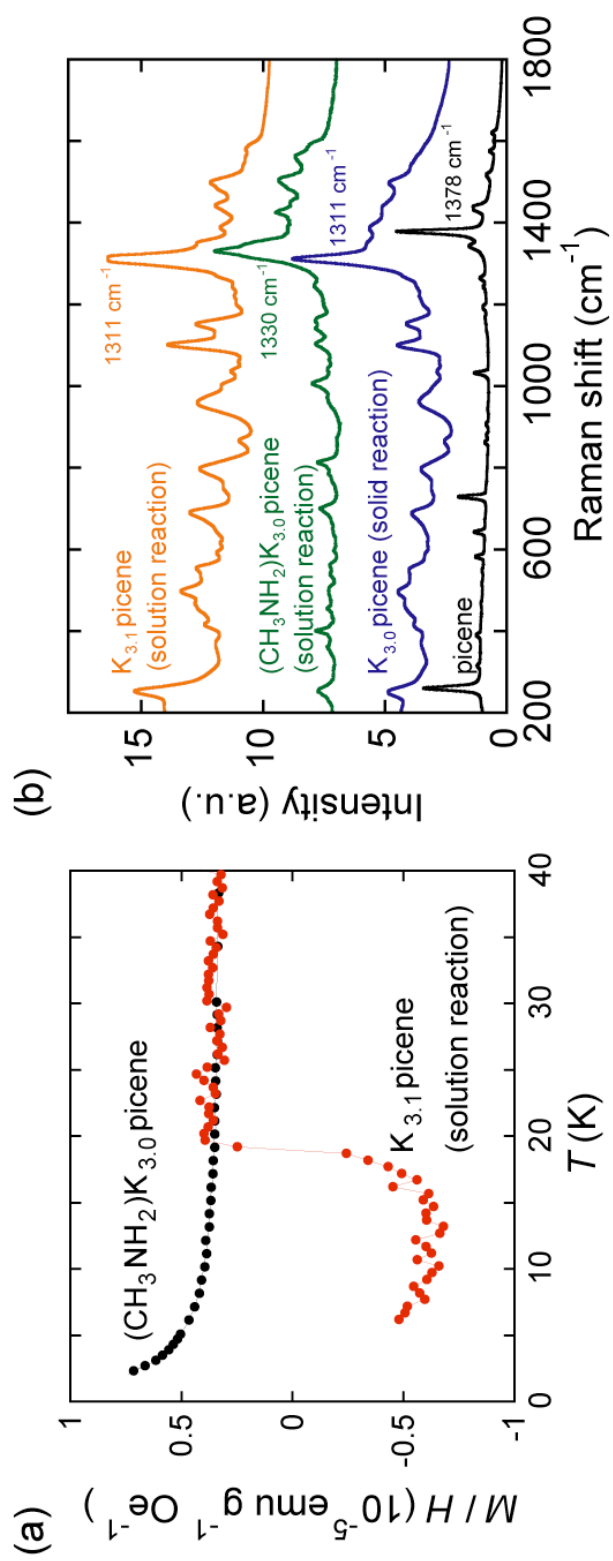


Figure 7. T. Kambe et al.,

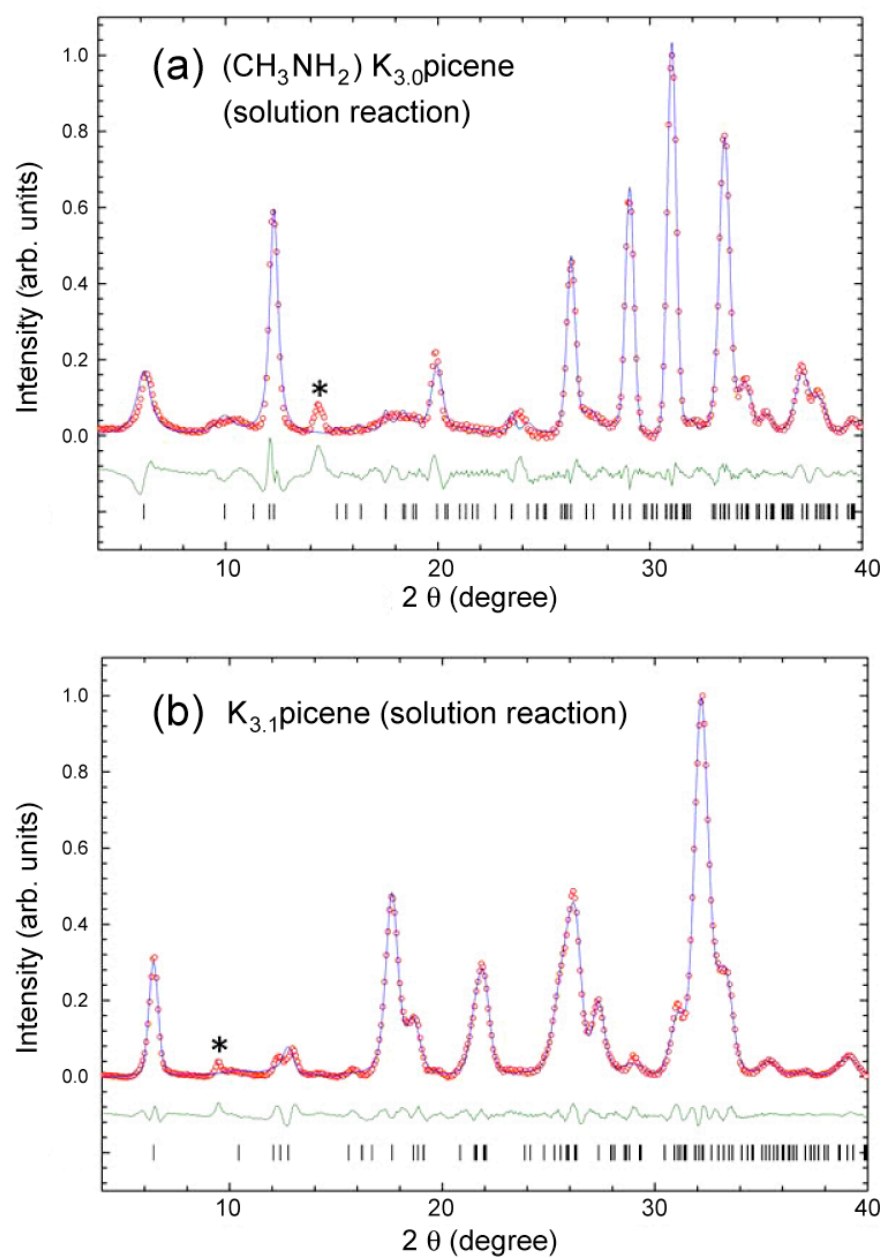


Figure 8. T. Kambe et al.,